CARBON 71 (2014) 338–342

Available at www.sciencedirect.com

ScienceDirect

journal homepage: www.elsevier.com/locate/carbon

Letter to the Editor

Improved conductivity of suspended carbon fibers through integration of C-MEMS and Electro-Mechanical Spinning technologies

G. Canton [a,*], T. Do [b], L. Kulinsky [a], M. Madou [a]

[a] Department of Mechanical and Aerospace Engineering, University of California, Irvine, 4200 Engineering Gateway, Irvine, CA 92697-3975, USA

[b] Division of Mathematics, Science and Engineering, Saddleback College, 28000 Marguerite Parkway, Mission Viejo, CA 92692, USA

ARTICLE INFO

Article history:
Received 26 September 2013
Accepted 6 January 2014
Available online 13 January 2014

ABSTRACT

Carbon microfibers suspended across carbon walls were fabricated by Electro-Mechanical Spinning and subsequent pyrolysis of a SU-8 based carbon precursor. The shrinkage and elongation of these polymer fibers during the pyrolysis process was observed to depend on the height of the supporting walls. We demonstrate that this shrinkage and elongation during pyrolysis strongly influences the resulting carbon electrical properties. Compared to fibers that retained their length during pyrolysis, conductivity was enhanced by a factor of seven after fibers were elongated four times their initial pre-pyrolysis length with a concurrent shrinkage of their diameter by half.

One-dimensional (1D) nanostructures such as nanotubes, nanowires, and nanofibers have unique physicochemical properties as compared to bulk structures making them excellent materials of choice for a wide variety of applications, including structural materials, analytical sensors and biosensors, as circuitry elements and interconnects in nanoelectronics and as components in microelectromechanical systems (MEMS). Among various materials for nanostructures, carbon has received significant attention due to its excellent electrical and thermal properties, low reactivity and wide electrochemical stability window that allows for numerous applications of carbon nanotubes (CNT) and carbon nanofibers. While significant progress has been achieved in the utilization of carbon nanofibers mats, one unmet need is the ability to produce precisely positioned carbon nanofibers with minimal contact resistance to the underlying substrates that might be flat (2D, fibers on the surface) or 3D (suspended fibers). Suspended carbon nanofibers of this kind, among many potential applications, can be used as micro/nano heating element allowing, for example, for inexpensive high sensitivity gas sensors [1]. Fabrication methods suitable for mass-production of these 1D suspended nanofibers should minimize the production costs and maximize the throughput. Promising carbon nanofibers manufacturing strategies such as Electron-Beam Lithography (EBL) or Dip-Pen Lithography (DPL) feature controlled writing of 1D nanostructures facilitating positioning and integration of individual nanofibers; however these technologies still face stiff economic and technical challenges for large-scale production. Combining electrospun carbon nanofibers with carbon-MEMS (C-MEMS) technology, Sharma et al. [2] have reported a successful low cost fabrication technique that suspends carbon

* *Corresponding author.*
E-mail address: cantong@uci.edu (G. Canton).
0008-6223/$ - see front matter
http://dx.doi.org/10.1016/j.carbon.2014.01.009

fibers across carbon microstructures. Indeed, electrospinning has emerged as a low-cost convenient method for fabricating various types of long continuous nanofibers, not only for low volume research and niche markets, but also for high volume industrial applications [3,4]. A first study on the conductivity of electrospun carbon nanofibers and its enhancement using CNT to increase the degree of graphitization was done by Maitra et al. [5]. Sharma et al. [6] also combined electrospinning and photolithography technologies to fabricate single suspended carbon nanofibers with increased graphitization to enhance their electrical conductivity. The latter authors suggested that the increased graphitization in their case was related to the mechanical pulling of the fibers during their deposition on a rotating collector drum. All those studies employed Far-Field Electrospinning (FFES) technology to deposit their nanofibers. In FFES a polymer jet is stretched in flight because of electrostatic forces and due to inherent electrical instabilities the fiber also makes a whipping motion. Because of the latter stochastic instability the resulting fibers cannot be individually positioned. Using FFES removal of unwanted fibers is often necessary using expensive and time consuming techniques such as Focus Ion Beam (FIB) [6].

To enhance nanofiber deposition control, we have developed Electro-Mechanical Spinning – EMS (also known as Low-Voltage Near-Field Electrospinning [7]). EMS achieves more stable and controllable fiber deposition by three main means: reduced distance between the electrodes (I), lower deposition voltage (II) and the utilization of highly visco-elastic polymer solutions (III). The reduction of the distance between the needle and the substrate electrodes allows the utilization of the stable liquid jet region for a controllable deposition and positioning of individual fibers. Secondly, lowering of the deposition voltage greatly reduces electrical instabilities resulting in a more controllable fiber jet. Finally, the utilization of a highly visco-elastic polymer solution allows for the mechanical thinning of the fiber jet without risk of premature breakage. Using EMS, continuous nanofibers with diameters ranging from microns to sub-20 nm were deposited onto 2D substrates and were also suspended between 3D structures (such as posts or walls) with high precision. A detailed description of the EMS setup and results on the fabrication of poly(ethylene oxide) (PEO) nanofibers with EMS were outlined in an earlier publication [7]. While PEO nanofibers cannot be pyrolized, SU-8 is a well-known carbon precursor and several recent works describe the optimization of EMS fabrication of SU-8 based carbon fibers suspended over C-MEMS structures [8,9]. Carbon electrodes fabricated using SU-8 as carbon precursor and the same pyrolysis conditions used in this study (see Supplementary data) have a conductivity of 8.2×10^3, typical of glassy carbon [10]. We expect that EMS carbon fibers have conductivity in this range, when not subjected to external alterations. Conductivity can be enhanced when graphitization and/or higher carbon structure alignment is induced, for example, by stretching and elongating the fibers during pyrolysis.

The present study aims to evaluate the electrical conductivity of suspended electro-mechanically spun fibers as a function of the difference in degree of fiber shrinkage and elongation during the carbonization process. Shrinkage and elongation depend strongly on the original height of the SU-8 walls supporting the fibers.

The basic precursor structures for the C-MEMS electrodes used as supports for EMS fiber deposition consist of two 100 μm wide, 3 mm long SU-8 walls, separated by a 20 μm gap. The four sets of wall heights utilized in this study are 20, 40, 60 and 80 μm (±3 μm). These structures are fabricated on top of a silicon wafer passivated with a 900 nm silicon dioxide insulating layer. A drawing, presenting microfabricated walls before and after carbonization is shown in Fig. 1. During the carbonization process the SU-8 walls structures lose their non-carbon atoms causing weight loss and volumetric shrinkage [11]. The upper portion of the suspending wall shrinks considerably more than the lower portion which is firmly anchored to the silicon dioxide substrate.

Using an SU-8 based polymer solution optimized for EMS [9] fifteen fibers per set of walls were then suspended and aligned 20 μm apart across the gap between the walls (Fig. 2). The resulting samples were then pyrolyzed at 900 °C in an inert (N_2) environment to carbonize fibers and supporting walls simultaneously.

Electro-mechanical spun fibers suspended over SU-8 walls undergo two types of mechanical pulling: mechanical pulling due to the movement of the substrate during fiber deposition (I) as well as pulling of the fibers during the carbonization process when the SU-8 walls, that are supporting the fibers, shrink (II). The wall's shrinkage increases the gap between the walls causing further stretching of the fibers.

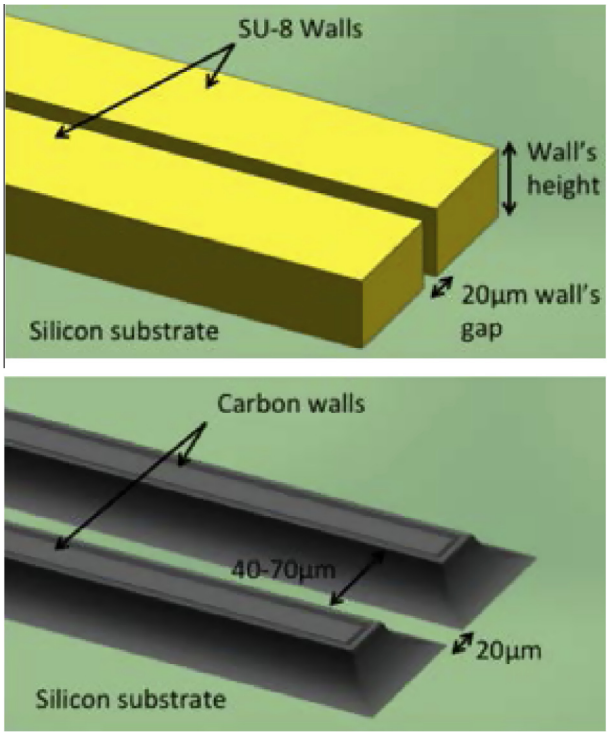

Fig. 1 – Schematic of the supporting walls structure. Top: lithographically patterned SU-8 (carbon precursor) walls. Bottom: walls after carbonization process.

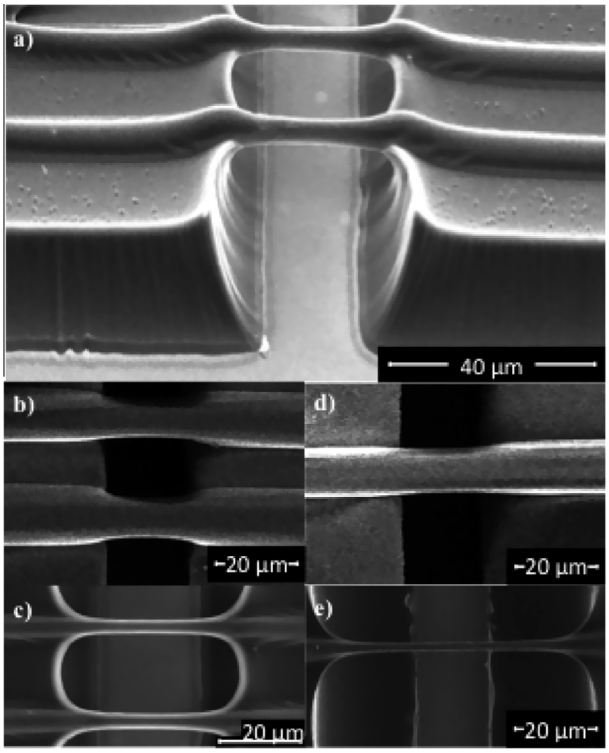

Fig. 2 – (a) SEM image (60° tilted view) of two carbon fibers suspended across the gap between supporting walls. Initial height of the walls: 20 μm. (b) Top view of the same fibers before pyrolysis. (c) Top view of the same fibers after pyrolysis. (d) SU-8 based fiber electromechanically spun across 80 μm high SU-8 walls (top view). (e) The fiber considered in (d) after pyrolysis (top view).

The higher the SU-8 structures, the more the upper parts of the walls shrink with respect to the bottom of the walls (see Fig. 1). A comparison between SEM images before and after pyrolysis of fibers suspended across 20 μm high SU-8 walls and across 80 μm high SU-8 walls is shown in Figs. 2b–e. The gap between the top of the two SU-8 walls is initially about 20 μm in both cases, but after carbonization that gap becomes about 40 μm for walls with an initial height of 20 μm (Fig. 2c) and about 70 μm for walls with an initial height of 80 μm (Fig. 2e).

We also deposited fibers across walls that were carbonized prior to fiber deposition. Since carbonized walls do not shrink during the subsequent pyrolysis (and thus do not provide additional pull on the fibers), we have included data from these pre-pyrolyzed walls in our study as control. The height of these carbonized walls is given as 0 μm to indicate the fact that there is no additional pull provided to the fibers during pyrolysis.

To quantify the shrinkage of the suspended fibers and its correlation with the fiber elongation during pyrolysis, the diameter and the length of the fibers were measured before and after pyrolysis using images taken with a Scanning Electron Microscope (FEI Quanta 3D FEG Dual Beam). Diameters are calculated from an average of 10 different measurements of the fiber width along the fiber length. The fiber elongation is calculated as: $E_{\%} = \frac{L_f - L_{in}}{L_{in}}$, where L_{in} and L_f are the average length of the fibers before and after pyrolysis respectively. Fig. 3a shows the elongation of the fibers at different initial wall heights and, as expected, the elongation of the fibers is larger for higher wall structures. However, the relationship is not linear and further increase in elongation of the fibers is no longer significant for walls with heights above 60 μm.

The fiber diameter shrinkage is calculated as: $D_{\%} = 1 - \frac{d_f}{d_{in}}$, where d_{in} is the initial diameter of the SU-8 based fibers before pyrolysis and d_f is the average diameter of the carbon fibers after pyrolysis. Results are graphed in Fig. 3b. The diameter of the fibers suspended over SU-8 walls shrinks compared to that of fibers suspended over pre-pyrolyzed walls (indicated by wall height of 0 μm on the graph). A slight diameter decrease is observed for a 20 μm wall height and a significant further diameter reduction is observed for a 40 μm wall. There is no significant difference in fiber diameter for fibers suspended over walls higher than 40 μm.

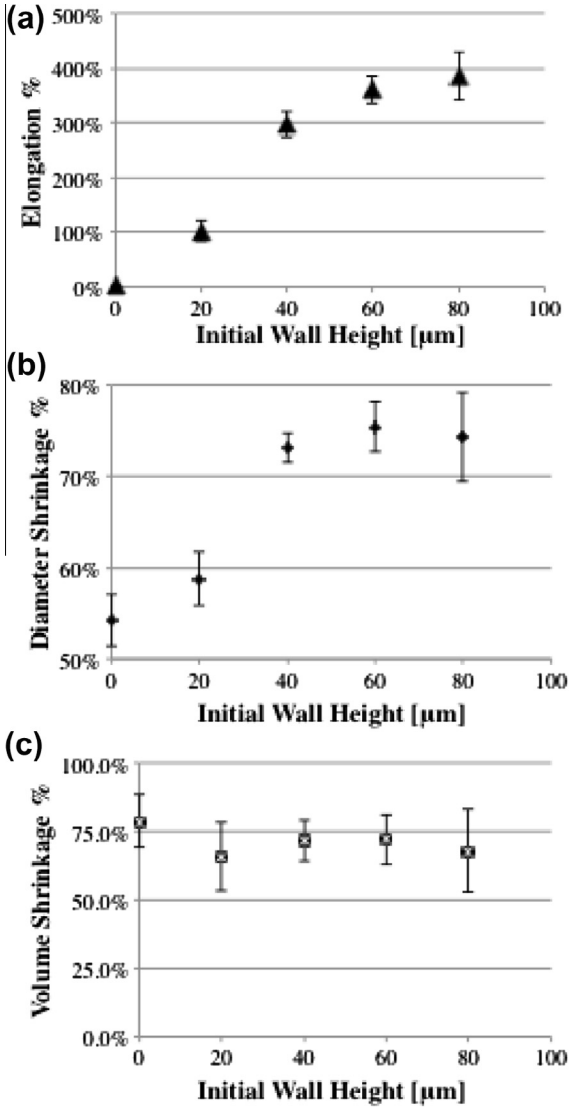

Fig. 3 – (a) Elongation, (b) diameter and (c) volume shrinkage are plotted vs. the initial structure thickness. Ten to twenty fibers have been measures per each data point. Error bars represent ± 2σ.

A possible explanation for the fact that fiber elongation and diameter shrinkage does not significantly further increase for walls higher than 40 μm is likely related to inability of the supporting walls to withstand higher tensile stresses since after pyrolysis we could observe cracks in the walls that are higher than 40 μm (see Supplementary data).

The volume shrinkage of the fiber is calculated as $V_{\%} = 1 - \frac{V_f}{V_{in}}$ (V_{in} and V_f are fiber volume pre- and post-pyrolysis respectively) and is graphed in Fig. 3c. There are no significant differences in terms of volume shrinkage among the various samples. This is expected because the carbon yield of the precursor material and the density of the final carbonized fiber are approximately the same for all the samples.

Fig. 4 shows an SEM image of that part of a suspended carbon fiber that is deposited on the top of the SU-8 wall. The morphology of the fiber surface suggests stresses in the fiber that encourage alignment of polymer chains along the fiber length. It is known that the mechanical pulling of SU-8 based electrospun fibers affects the resulting carbon structure post-pyrolysis by enhancing graphitization along the pulling direction [6].

In order to check if enhanced graphitization indeed takes place because of mechanical pulling of the precursor fiber, we investigated the electrical conductivity of carbon fibers suspended across walls of different heights (same as Fig. 3). For this purpose nine samples with a single fiber bridging a gap between walls of different heights were fabricated under the same Electro-Mechanical Spinning conditions. The average diameter of those nine fibers was 3.9 μm ± 0.2 μm before pyrolysis. The *I*–*V* curves for each fiber after pyrolysis were generated using an impedance analyzer (Keithley 428) connected to the carbon walls close to the suspended carbon fiber using a micro-probe station. The obtained *I*–*V* curves were linear confirming the Ohmic nature of the carbon–carbon contact between fibers and wall structures.

Fig. 5a shows the conductivity vs. the initial wall height. The trend is similar to the one seen for the elongation % and shrinkage % in Fig. 3. In Fig. 5b the conductivity is plotted vs. the final thickness of the fiber after pyrolysis. In both graphs the red line represents the conductivity of carbon electrodes pyrolized from SU-8 under the same pyrolysis conditions as the fibers in the study. Fibers that underwent minimal stretching during pyrolysis have conductivity values

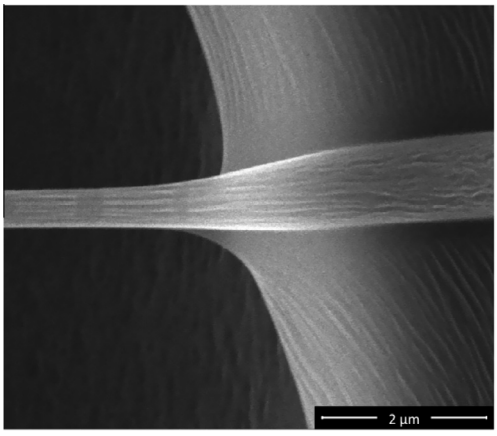

Fig. 4 – SEM image of a section of a suspended carbon fiber.

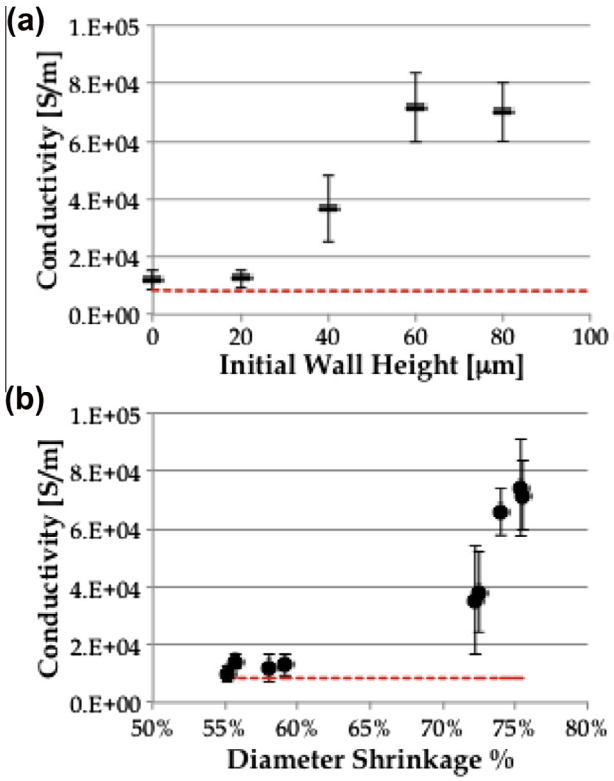

Fig. 5 – (a) Conductivity vs. initial wall height; (b) conductivity vs. fiber thickness after pyrolysis. Error bars represent ± 2σ.

very close to that of the SU-8 based carbon electrodes, while fibers that experienced high degree of shrinkage have a higher electrical conductivity. This points out that those highly stretched carbon fibers might not be purely glassy carbon, but might have some degree of graphitization (conductivity of the graphite is between 2×10^5 and 3×10^5 S/m when aligned parallel to the fiber direction).

In this study we employed relatively low cost micro-fabrication technologies to individually position SU-8 fibers across lithographically defined SU-8 walls. The fibers and the walls were then carbonized leading to a unified structure with negligible contact resistance. The study focused on the characterization of the suspended fibers before and after the carbonization process quantifying the shrinkage and elongation phenomena that occur during and their relationship with fiber conductivity. Higher supporting walls led to thinner and more elongated fibers post-pyrolysis. It was demonstrated that the conductivity of the fibers increases with the amount of elongation and concurrent diameter reduction, consistent with the hypothesis that structural alignment imposed during deposition of the fiber and subsequent pyrolysis leads to higher degree of graphitization.

Acknowledgements

The authors are grateful to Dr. Horacio Kido, RotaPrep, Inc., for the EMS equipment; to Prof. Philip G. Collins for the use of the equipment for conductivity characterization and

Mr. Elliot J. Fuller for the technical assistance and support; to Integrated Nanosystems Research Facility (INRF) at University of California, Irvine for the use of microfabrication equipment. SEM work was performed at the Laboratory for Electron and X-ray Instrumentation (LEXI) at UC Irvine, using instrumentation funded in part by the National Science Foundation Center for Chemistry at the Space-Time Limit (CHE-082913).

Appendix A. Supplementary data

Supplementary data associated with this article can be found, in the online version, at http://dx.doi.org/10.1016/j.carbon.2014.01.009.

REFERENCES

[1] Sharma S, Madou M. A new approach to gas sensing with nanotechnology. Philos Trans R Soc A: Math, Phys Eng Sci 1967;2012(370):2448–73.
[2] Sharma CS, Katepalli H, Sharma A, Madou M. Fabrication and electrical conductivity of suspended carbon nanofiber arrays. Carbon 2011;49(5):1727–32.
[3] Doshi J, Reneker DH. Electrospinning process and applications of electrospun fibers. J Electrostat 1995;35(2):151–60.
[4] Persano L, Camposeo A, Tekmen C, Pisignano D. Industrial upscaling of electrospinning and applications of polymer nanofibers: a review. Macromol Mater Eng 2013;298(5):504–20.
[5] Maitra T, Sharma S, Srivastava A, Cho Y-K, Madou M, Sharma A. Improved graphitization and electrical conductivity of suspended carbon nanofibers derived from carbon nanotube/polyacrylonitrile composites by directed electrospinning. Carbon 2012;50(5):1753–61.
[6] Sharma S, Sharma A, Cho YK, Madou M. Increased graphitization in electrospun single suspended carbon nanowires integrated with carbon-MEMS and carbon-NEMS platforms. ACS Appl Mater Interfaces 2012;4(1):34–9.
[7] Bisht GS, Canton G, Mirsepassi A, Kulinsky L, Oh S, Dunn-Rankin D, et al. Controlled continuous patterning of polymeric nanofibers on three-dimensional substrates using low-voltage near-field electrospinning. Nano Lett 2011;11(4):1831–7.
[8] Canton G, Bisht G, Kulinsky L, Madou M. Controlled patterning and dimensional control of suspended carbon nanofibers. Adv Mater Res 2013;628:43–9.
[9] Canton G, Kulinsky L, Madou MJ. Electro-Mechanical Spinning: A new manufacturing technique for micro/nano-fabrication of carbon fibers. Advanced Packaging Materials (APM), 2013 IEEE International Symposium on: IEEE; p. 230–9.
[10] Mardegan A, Kamath R, Sharma S, Scopece P, Ugo P, Madou M. Optimization of carbon electrodes derived from epoxy-based photoresist. J Electrochem Soc 2013;160(8):B132–7.
[11] Park BY, Taherabadi L, Wang C, Zoval J, Madou MJ. Electrical properties and shrinkage of carbonized photoresist films and the implications for carbon microelectromechanical systems devices in conductive media. J Electrochem Soc 2005;152(12):J136–43.